Independent modeling of fluorescence excitation and emission with the finite element method

Ralf B. Schulz, Jörg Peter and Wolfhard Semmler
Dept. Medical Physics in Radiology, German Cancer Research Center,
Im Neuenheimer Feld 280, 69120 Heidelberg, Germany
r.schulz@dkfz.de

Wolfgang Bangerth
Center for Subsurface Modeling, Institute for Computational Engineering and Sciences, The University of Texas at Austin,
201 East 24th Street, ACE 5.324, Austin, TX 78712

Abstract: Based on the diffusion equation, a parallel FEM system is proposed, describing photon propagation and fluorescence emission using appropriate boundary conditions. Iterative reconstruction methods will benefit from the speed-up due to parallelized forward model execution.

OCIS codes:

1. Introduction

Fluorescence tomographic methods aim at reconstructing the concentration of fluorophores within the imaged object. Diffuse measurements of fluorescence emissions are obtained on the boundary of the object; excitation is performed through external laser sources at various positions. These methods become increasingly important in the context of targeted or activatable fluorescent probes, "smart" contrast agents with merely no background that offer unique functional imaging capabilities on the cellular or sub-cellular level. Spatially resolved quantification of fluorochrome concentration could provide a measure for receptor concentration, gene expression or enzymatic activity, depending on the probe used [1]. While this method is commonly employed in the field of fluorescence microscopy, the necessary means to quantitatively image small animals are just being developed. Due to the excellent signal to background ratio, sub-millimeter resolution in homogeneous phantoms is reported [2].

An established standard model for photon propagation in turbid media is the time-independent diffusion equation, derived from the radiative transfer equation [3]. It is less computationally expensive, but is not valid in all biological environments [4]. The photon density created by a continuous source emitting at wavelength λ described by an input function $q(\mathbf{r})$ within a turbid domain Ω of inhomogeneous absorption and scattering properties $\mu_{a\lambda}$ and $\mu_{s\lambda}'$ can be approximated by the following diffusion equation, describing the photon fluence Φ using coefficients $\mu_{a\lambda}$ and $D_\lambda = \left[3\left(\mu_{s\lambda}'+\mu_{a\lambda}\right)\right]^{-1}$ for absorption and diffusion, respectively:

$$\left(-\nabla D\nabla + \mu_a(\mathbf{r})\right)\Phi(\mathbf{r}) = q(\mathbf{r}), \quad \mathbf{r}\in\Omega \tag{1}$$

Internal reflection at the boundaries $\partial\Omega$ can be modeled with Robin boundary conditions of the form:

$$\Phi(\mathbf{r}_b) + 2AD\mathbf{n}\cdot\nabla\Phi(\mathbf{r}_b) = 0, \quad \mathbf{r}_b\in\partial\Omega, \quad A = \frac{2/(1-R_0)-1+|\cos\theta_c|^3}{1-|\cos\theta_c|^2}, \tag{2}$$

where A describes reflection due to refractive index mismatch of object and surrounding non-scattering medium [5]. External, collimated sources cannot be described by (1) and (2) directly, but are usually approximated by point sources $q(\mathbf{r}) = \Theta_s\delta_0(\mathbf{r}-\mathbf{r}_s)$ of power Θ_s one diffusion length away from the boundary into the medium [6]. For biomedical applications it is generally assumed that only external sources are present for excitation while internal sources represent fluorescence.

With respect to the coefficients, the diffusion equation of (1) and (2) can be linearized and then inverted [2,7] employing Green's functions and a small perturbation approach. While this results in a linear system quickly solvable with standard methods, the solution is disturbed by inhomogeneities of the domain [8,9]. Furthermore, the implementation of boundary conditions (2) is complex and time-consuming, although new approximations have been published recently [10]. The finite element method, however, is capable of modeling the system (1) and (2) accurately, but only the forward problem can be solved easily. Parameter estimation is performed using non-linear methods that usually require a large number of forward calculations [11,12]. We present herein a way to reduce the computational effort for a combined model describing fluorescence and absorption by decoupling the underlying system of equations.

2. Independent formulation of excitation and emission

Fluorochromes within domain Ω increase the absorption at λ by $\varepsilon_\lambda c(\mathbf{r})$, where c is the spatially varying concentration and ε_λ is the molar extinction coefficient of the fluorochrome at wavelength λ. The fluorochrome will emit at a wavelength λ' with a probability of $\gamma_{\lambda'}$, the quantum yield, which is regarded as spatially invariant. Assuming that only two distinct wavelengths are present—excitation wavelength λ_x and emission wavelength λ_m—results in the coupled equations:

$$\begin{aligned} \left(-\nabla D_x \nabla + \mu_{ax}(\mathbf{r}) + \varepsilon_x c(\mathbf{r})\right) \Phi_x(\mathbf{r}) &= \Theta_s \delta_0(\mathbf{r}-\mathbf{r}_s) \\ \left(-\nabla D_m \nabla + \mu_{am}(\mathbf{r})\right) \qquad\quad \Phi_f(\mathbf{r}) &= \gamma_m \varepsilon_x c(\mathbf{r}) \Phi_x(\mathbf{r}) \end{aligned} \tag{3}$$

Under the assumption that the Stokes shift is small, the equality of the coefficients for both wavelengths can be considered equal, i.e. $D_x = D_m = D$ and $\mu_{ax} = \mu_{am} = \mu_a$. Also, ε and γ can be written without index. The first equation in (3) can then be rewritten as

$$\varepsilon c(\mathbf{r}) \Phi_x(\mathbf{r}) = \Theta_s \delta_0(\mathbf{r}-\mathbf{r}_s) - \left(-\nabla D \nabla + \mu_a(\mathbf{r})\right) \Phi_x(\mathbf{r}). \tag{4}$$

Substituting (4) in (3) and dividing by γ, this yields

$$\begin{aligned} \left(-\nabla D \nabla + \mu_a(\mathbf{r}) + \varepsilon c(\mathbf{r})\right) \Phi_x(\mathbf{r}) &= \Theta_s \delta_0(\mathbf{r}-\mathbf{r}_s) \\ \left(-\nabla D \nabla + \mu_a(\mathbf{r})\right) \qquad \left(\tfrac{1}{\gamma}\Phi_f(\mathbf{r}) + \Phi_x(\mathbf{r})\right) &= \Theta_s \delta_0(\mathbf{r}-\mathbf{r}_s), \end{aligned} \tag{5}$$

which is solved with respect to $\Phi_t = \frac{1}{\gamma}\Phi_f + \Phi_x$. This way, both equations become independent and can be computed completely in parallel, thus decreasing the total computation time needed for one forward solution by one half. The fluence rate due to fluorescence is recovered by calculating $\Phi_f = \gamma(\Phi_t - \Phi_x)$ afterwards, if desired. In an experimental setting, measurements are taken at the boundary at both wavelengths through the use of filters, so that boundary measurements $\hat{\Phi}_x, \hat{\Phi}_m$ can easily be combined to $\hat{\Phi}_t = \frac{1}{\gamma}\hat{\Phi}_f + \hat{\Phi}_x$ and used in an error estimator or measurement operator.

3. Finite Element Formulation

A solution for (5) can be obtained by using a Galerkin approach, which yields the weak formulation of the problem, similar to the models used in [6,12][1]:

$$\begin{aligned} \left(\nabla\varphi_i, D\nabla\Phi_x\right)_\Omega + \left(\varphi_i, (\mu_a + \varepsilon c)\Phi_x\right)_\Omega - \left(\varphi_i, \tfrac{1}{2AD}\Phi_x\right)_{\partial\Omega} &= \Theta_s \varphi_i(\mathbf{r}_s) \\ \left(\nabla\psi_i, D\nabla\Phi_t\right)_\Omega + \left(\psi_i, \mu_a \Phi_t\right)_\Omega \qquad - \left(\psi_i, \tfrac{1}{2AD}\Phi_t\right)_{\partial\Omega} &= \Theta_s \psi_i(\mathbf{r}_s), \end{aligned} \tag{6}$$

for all test functions φ_i and ψ_i, where $(a,b)_\Omega = \int_\Omega a(\mathbf{r}) b(\mathbf{r}) d\mathbf{r}$ is the scalar product on the full domain Ω and $(a,b)_{\partial\Omega} = \int_{\partial\Omega} a(\mathbf{r}) b(\mathbf{r}) d\mathbf{r}$ is the scalar product on its boundary $\partial\Omega$. Setting $\Phi_s = \sum_j \alpha_j \varphi_j, \alpha_j \in \mathbb{R}$ and $\Phi_t = \sum_j \beta_j \psi_j, \beta_j \in \mathbb{R}$, the left hand side of (6) turns into a matrix-vector equation where the vector contains the unknown coefficients α and β while the matrix contains the scalar products only depending on the test functions. For an appropriate choice of functions, the matrix is sparse and the equation can be inverted quickly, resulting in a solution for α and β. The solution to (6) equals a projection of Φ_x and Φ_t into the space of test functions. The resulting equations in matrix form are:

$$\begin{aligned} \left(\mathbf{D}_\varphi + \mathbf{A}_\varphi + \varepsilon \mathbf{c}_\varphi - \mathbf{B}_\varphi\right)\boldsymbol{\alpha} &= \Theta_s \left[\varphi_i(\mathbf{r}_s)\right] \\ \left(\mathbf{D}_\psi + \mathbf{A}_\psi \qquad - \mathbf{B}_\psi\right)\boldsymbol{\beta} &= \Theta_s \left[\varphi_i(\mathbf{r}_s)\right] \end{aligned} \tag{7}$$

Note that if the same function spaces are used, the system matrices are nearly similar and could also be computed just once, with later addition of $\varepsilon \mathbf{c}_\varphi$ for the first equation.

We implemented a finite element system based on the freely available DEAL-II library (www.dealii.org) [13]. The library uses hexahedral meshes that can be employed in a dimension-independent way. For exemplary purposes, a three-dimensional cylindrical mesh of 4cm diameter and 4cm length with background properties $\mu_a = 0.3 cm^{-1}$ and $\mu_s' = 10 cm^{-1}$ was used with a point source located at one diffusion length away from the border of the domain (Fig.1). Boundary conditions were applied to the outer part of the cylinder, with the exception of top and bottom

side. These boundaries were left floating to simulate an infinite cylinder. A spherical fluorescent emitter with diameter 2mm and μ=0.19cm^{-1} and γ=0.23 was simulated at different distances from the source (Fig.2). The properties of this emitter resemble a 1μM solution of fluorochrome Cy5.5 (Amersham Biosciences).

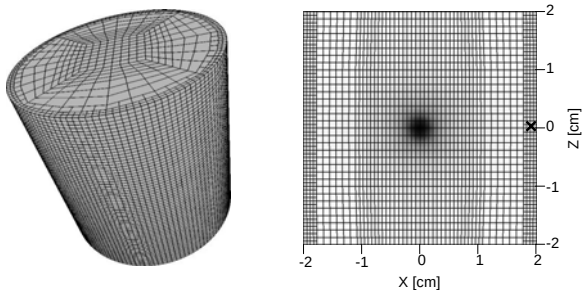

Fig. 1: The cylindrical mesh consisting of hexahedrals is shown on the left. The cylinder was 4cm long and had a diameter of 4cm. The outer layers were more refined to account for correct source modelling. The fluence created by a fluorescent source with μ=0.19cm^{-1} and γ=0.23 excited by a source on the right side (cross) is shown in a central slice along the cylinders main axis, after subtraction of the source fluence from the result of Eq. (5). Relative insensity is shown on a linear greyscale.

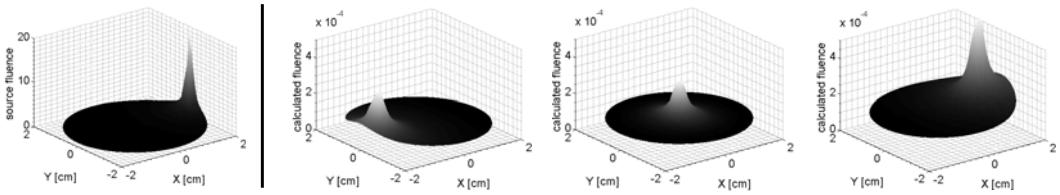

Fig. 2: Predicted fluence of the source (left) and of the fluorochrome at different positions (left to right): opposite rim, center, close to the source. Slices were taken from the center of the cylinder, at z=0.

4. Discussion

While the assumption of small changes in the optical parameters for a small shift in wavelength is generally accepted and frequently made, the idea of a spatially invariant quantum yield might be questionable in biological environments. However, newly developed anorganic emitters like quantum dots which are embedded in an isolator, are independent of the environment [14]. Also, a constant quantum yield is a basic assumption of quantitative fluorescence imaging as in [2] or in [15]. Thus, we propose to implement a non-linear iterative reconstruction based on the new, faster forward model. It might also be advantageous to estimate the system parameters of the governing equation of Φ_t in (6), as it is independent of fluorochrome concentration, and then estimate the concentration in a second iteration.

[1] R. Weissleder, V. Ntziachristos, "Shedding light onto live molecular targets," Nat Med **9**, 123–128 (2003).
[2] E.E. Graves, J. Ripoll, R. Weissleder, V. Ntziachristos, "A sub-millimeter resolution fluorescence molecular imaging system for small animal imaging," Med Phys **30**, 901–911 (2003).
[3] S.R. Arridge, "Optical tomography in medical imaging," Inv Probl **15**, R41–R93 (1998).
[4] A.H. Hielscher, R.E. Alcouffe, R.L. Barbour, "Comparison of finite-difference transport and diffusion calculations for photon migration in homogeneous and heterogeneous tissues," Phys Med Biol **43**, 1285–1302 (1998).
[5] M. Keijzer, W.M. Star, P.R. Storchi, "Optical diffusion in layered media," Appl Opt **27**, 1820–1824 (1988).
[6] M. Schweiger, S.R. Arridge, M. Hiraoka, D.T. Delpy, "The finite element method for the propagation of light in scattering media: Boundary and source conditions," Med Phys **22**, 1779–1792 (1995).
[7] V. Ntziachristos, R. Weissleder, "Experimental Three-Dimensional Fluorescence Reconstruction of Diffuse Media by use of a Normalized Born Approximation," Opt Lett **26**, 893–895 (2001).
[8] H. Dehghani, B.W. Pogue, J. Shudong, B. Brooksby, K.D. Paulsen, "Three-dimensional optical tomography: resolution in small-object imaging," Appl Opt **42**, 3117–3128 (2003).
[9] V. Ntziachristos, A.H. Hielscher, A.G. Yodh, B. Chance, "Diffuse optical tomography of highly heterogeneous media," IEEE Trans Med Im 20, 470–478 (2001).
[10] J. Ripoll and V. Ntziachristos, "An iterative boundary reflection method for diffuse optical tomography," JOSA A **20**, 1103–1110 (2003).
[11] A. Klose, A. Hielscher, "Quasi-Newton methods in optical tomographic image reconstruction," Inv Prob **19**, 387–409 (2003).
[12] R. Roy, E.M. Sevick-Muraca, "Truncated Newton's optimization scheme for absorption and fluorescence optical tomography: Part I theory and formulation," Opt Exp **4**, 353–371 (1999).
[13] W. Bangerth, R. Rannacher, *Adaptive Finite Element Methods for Differential Equations* (Birkhäuser, Basel, 2003).
[14] J.K. Jaiswal, H. Mattoussi, J.M. Mauro, S.M. Simon, "Long-term multiple color imaging of live cells using quantum dot bioconjugates," Nat Biotech **21**, 47–51 (2003).
[15] A.B. Milstein, S. Oh, K.J. Webb, C.A. Bouman, Q. Zhang, D.A. Boas, and R.P. Millane, "Fluorescence optical diffusion tomography," App Opt **42**, 3081–3094 (2003).